

# NJC

Accepted Manuscript



This is an *Accepted Manuscript*, which has been through the Royal Society of Chemistry peer review process and has been accepted for publication.

*Accepted Manuscripts* are published online shortly after acceptance, before technical editing, formatting and proof reading. Using this free service, authors can make their results available to the community, in citable form, before we publish the edited article. We will replace this *Accepted Manuscript* with the edited and formatted *Advance Article* as soon as it is available.

You can find more information about *Accepted Manuscripts* in the [Information for Authors](#).

Please note that technical editing may introduce minor changes to the text and/or graphics, which may alter content. The journal's standard [Terms & Conditions](#) and the [Ethical guidelines](#) still apply. In no event shall the Royal Society of Chemistry be held responsible for any errors or omissions in this *Accepted Manuscript* or any consequences arising from the use of any information it contains.

## Nonsymmetric dimers comprising chalcone and cholesterol entities: An investigation on structure-property correlations

Ammathnadu S. Achalkumar,<sup>\*a</sup> Doddamane S. Shankar Rao<sup>b</sup>, and Channabasaveshwar V. Yelamaggad<sup>\*b</sup>

<sup>a</sup>Indian Institute of Technology Guwahati, Guwahati, 781039, Assam, India

<sup>b</sup>Centre for Soft Matter Research, Jalahalli, P. B. No. 1329, Bangalore, 560013, India.

**Abstract:** Four series of new dimers formed by interlinking chalcone and cholesterol mesogenic entities through a spacer of varying length and parity have been synthesized and characterized by polarizing optical microscope, differential scanning calorimeter, X-ray diffraction and electrical switching studies. Structure of the chalcone core has been systematically modified to investigate the effect of the molecular structure on the thermal behaviour of dimers. The study demonstrates the dramatic dependence of thermal behaviour of these dimers on the nature of the chalcone besides the length and parity of the spacer.

### I. Introduction

Liquid crystal (LC) phases formed by the self-assembly of shape anisotropic molecules (mesogens) represent a distinct and unique state of matter.<sup>1</sup> Since their discovery,<sup>2</sup> they have been attracting attention as they combine order of the solids and mobility of liquids at the molecular and mesoscopic levels.<sup>1</sup> The chiral LC phases, resulting from entirely chiral mesogens or by doping the LC phase with a suitable chiral dopant, are fascinating as they exhibit novel structures and special properties that are promising in the arenas of both basic and applied research;<sup>3-5</sup> while the helical superstructures of the chiral nematic (N\*) or chiral smectic C (SmC\*) have been recognized as media for device applications,<sup>3</sup> the frustrated phases such as blue phases (BPs) and twist grain boundary (TGB) phases have generated great interest owing to their complex structures.<sup>4,6</sup> Three types of blue phases viz., BPI, BPII and BPIII are known to exist that comprise double twist cylinders, as shown in Fig. 1a. Generally, BPs exist over a short thermal range between the N\* / smectic (Sm) phase and the isotropic liquid (I) phase. Owing to their huge promise in transmissive<sup>6a,b</sup> and reflective displays,<sup>6c-e</sup> and photonics applications,<sup>6f-i</sup> there have been efforts to widen the thermal stabilities of these phases.<sup>6j,k</sup> Similar to BPs, TGB phases occur over a short thermal range at the phase transition from the I / N\* to smectic A (SmA) or chiral smectic (SmC\*) phases. Although their importance in applied science is not revealed hitherto, they have attracted attention being regarded as LC analogues of the Abrikosov phases exhibited by type-II superconductors. Three main types of TGB

phases are the TGBA, TGBC and TGBC\* where the slabs have orthogonal smectic A (SmA), tilted smectic C (SmC) and helical SmC\* characters respectively. As representative cases, the structures of TGBA and TGBC\* are shown in Fig. 1d-e

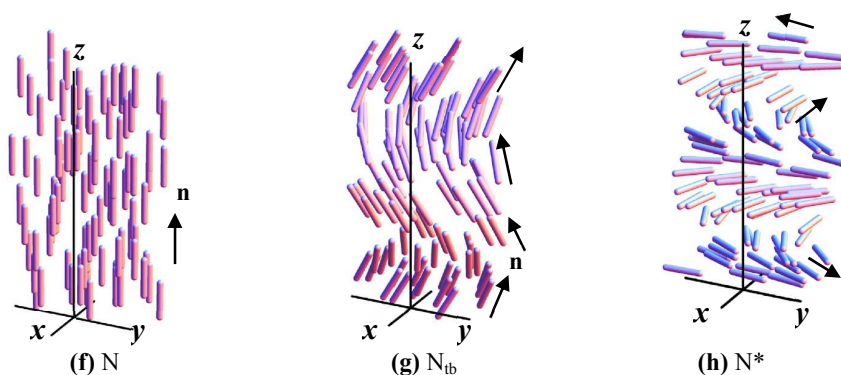
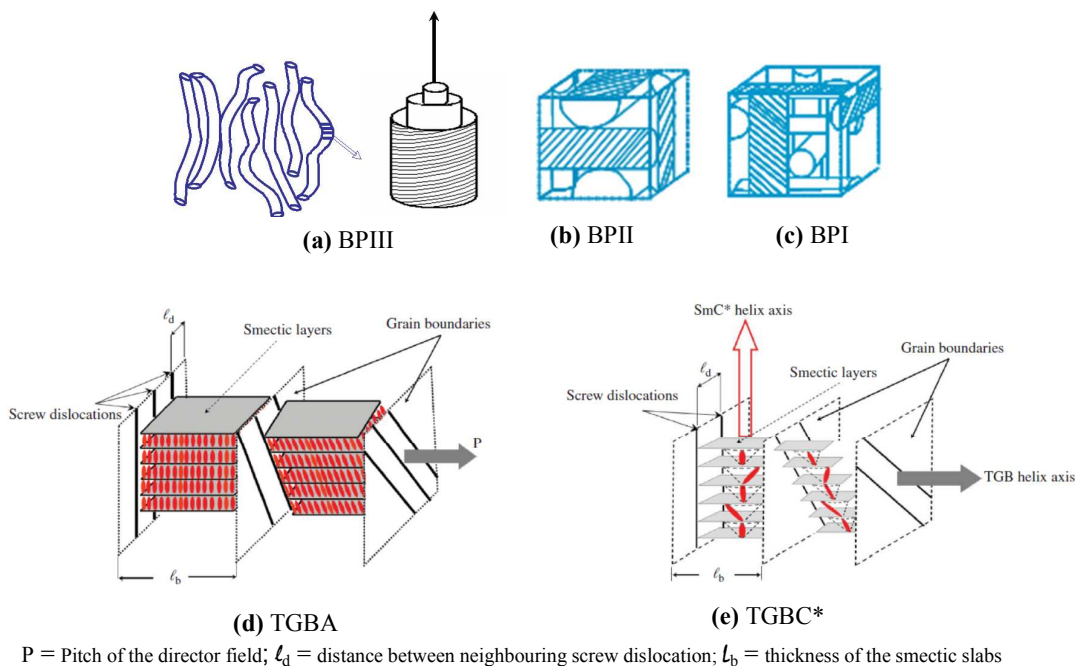


Figure 1: Schematic illustration of the molecular arrangement in the frustrated phases (a)The spaghetti model representation of BPIII phase (left portion) having randomly oriented squirming double twist tubes (right portion). Spatial arrangement of the double twist cylinders in the (b) simple cubic structure of BPII and (c) body centred cubic structure of BPI. (d) TGBA and (e) TGBC\* phases. Disposition of the molecules in the (f) N phase where the director,  $\mathbf{n}$ , is uniform globally, (g)  $N_{tb}$  phase with the local director following oblique helicoids and (h)  $N^*$  phase wherein the local director is normal to the helical axis,  $z$ . (Figs 1d-e are reprinted with permission from ref. 15k; Figs 1f-1h are reprinted with permission from ref. 8)

In recent years, liquid crystalline dimers composed of either two identical (symmetrical) or non-identical (nonsymmetrical) mesogens interlinked through a flexible spacer have been investigated intensively not only because they serve as model systems for polymeric LCs but also due to their remarkable thermal behaviour exhibiting odd-even effect, new LC phases, unprecedented phase sequences, frustrated phases etc.<sup>7-15</sup> For example, symmetric dimers are known to exhibit a rich smectic polymorphism besides showing an archetypal spacer-parity directed odd-effect.<sup>7</sup> Recently, one of the most remarkable phase transitional property of such symmetric, achiral dimers with an odd-numbered spacer has been disclosed;<sup>8</sup> the occurrence of a new twist-bend nematic ( $N_{tb}$ ) phase, which signifies a structural correlation among the well-known uniaxial nematic (N) and the  $N^*$  phases, has been reported (Fig. 1f-h). Notably, this new nematic order is non-layered, polar and structurally chiral, although the constituent mesogens themselves are achiral. In fact, in this phase, the constituent molecules self-assemble to form a helical structure and unlike in the  $N^*$  phase, the local director ( $\mathbf{n}$ ) (a preferred orientational direction of mesogens) is not perpendicular to the helix axis but forms an angle that depends on the magnitude of the spontaneous bend and the twist elastic constant. Interestingly, there have been speculations about the correlations between the  $N_{tb}$  structure and double-twist structure of the BPs formed by LC dimers.<sup>6j</sup> Thus, symmetric dimers are turning out to be interesting materials

Likewise, non-symmetric dimers, especially the chiral systems formed by tethering pro-mesogenic cholesterol to one of the termini of rod-like mesogen via a flexible spacer of varying length and parity, exhibit significant phase transitional properties.<sup>10</sup> For example, different types of frustrated structures, re-entrant phenomenon and unprecedented sequences have been observed in these materials. They show critical dependence of transition temperatures and enthalpies on the parity of the central flexible spacer. Their behaviour is also governed by the relative lengths of spacer and terminal tail as well as the chemical nature of the rod-like (non-cholesteryl) mesogen attached to cholesterol. It is shown that using appropriate combination of these chemical parameters one can modulate the physical properties of technologically important LC phases.<sup>10</sup> Although the LC behaviour of a large number of cholesterol-based dimers belonging to different series are accumulated, a complete understanding of the structure-property correlation is still

difficult as subtle modifications to the molecular structure bring about a drastic change in the LC property.<sup>10</sup>

These observations prompted us to design and synthesize cholesterol-based non-symmetric dimers with variation in the molecular structure of aromatic mesogenic unit and the length (and parity) of the central spacer. For example, there have been some interesting reports on such dimers where the significance of non-chiral aromatic segments such as Schiff's base, salicylaldehyde, azobenzene, stilbene, tolan, biphenyl, sydnone, chalcone, oxadiazole or cinnamate units has been well demonstrated.<sup>11-15</sup> Among these, the chalcone unit, where two phenyl rings are interconnected through an  $\alpha,\beta$ -unsaturated carbonyl group, being small bent-core, found to enhance the chirality of the dimers when connected to cholesterol through a spacer.<sup>15h,i</sup> From the point of material sciences, they have gained prominence as non-linear optically active (NLO) materials with excellent blue-light transmittance and good crystallizability.<sup>16</sup> With two planar rings connected through a conjugated double bond, they provide the necessary configuration to display NLO property. 4,4'-Difluoro-chalcone is especially used in the synthesis of NLO active polymers.<sup>17</sup> Prompted by these observations and in continuation of our quest to synthesize novel dimeric materials we chose to incorporate chalcone as the non-cholesteryl mesogen in the cholesterol-based dimeric structure. In view of the fact that the majority of the dimers realized earlier by our group derived from chalcone-cholesterol combination (see Chart 1, **4DC-n,m** series) exhibit frustrated phases over a wide thermal range,<sup>15h,i</sup> we were inspired to undertake a systematic investigation on analogous dimers to possibly understand the correlation between molecular structure and thermal properties. As possible modifications to the parent series, we prepared as many as four (1 to 4) series of dimers; the general molecular structures of four series dimers are shown in Chart 1. While the length of terminal tail was varied in the first series, the length and parity of the central  $\omega$ -oxyalkanoyl spacer were varied commonly in all series of dimers.

At the start, we altered the position of attachment of the spacer to the mesogenic (non-cholesteryl) segment; that is, a homologous series of dimers were prepared (Series 1: **3DC-n,m**) by *o*-alkylating 4-*n*-alkoxy-3'-hydroxy chalcones with cholesteryl  $\omega$ -bromoalkanoates. Given the fact that the  $\alpha,\beta$ -unsaturated carbonyl group

of the chalcone unit is a polar, we reversed the position of such a group that possibly inverts the direction of the polarity of the dimers. This alteration resulted in dimers of Series 2 (**3RDC-n** series) where the substitution of terminal chain is at 3-position with respect to carbonyl moiety attached to terminal phenyl ring. The increase in the length of the aromatic (phenyl) ring by attaching another phenyl ring, promotes the lateral

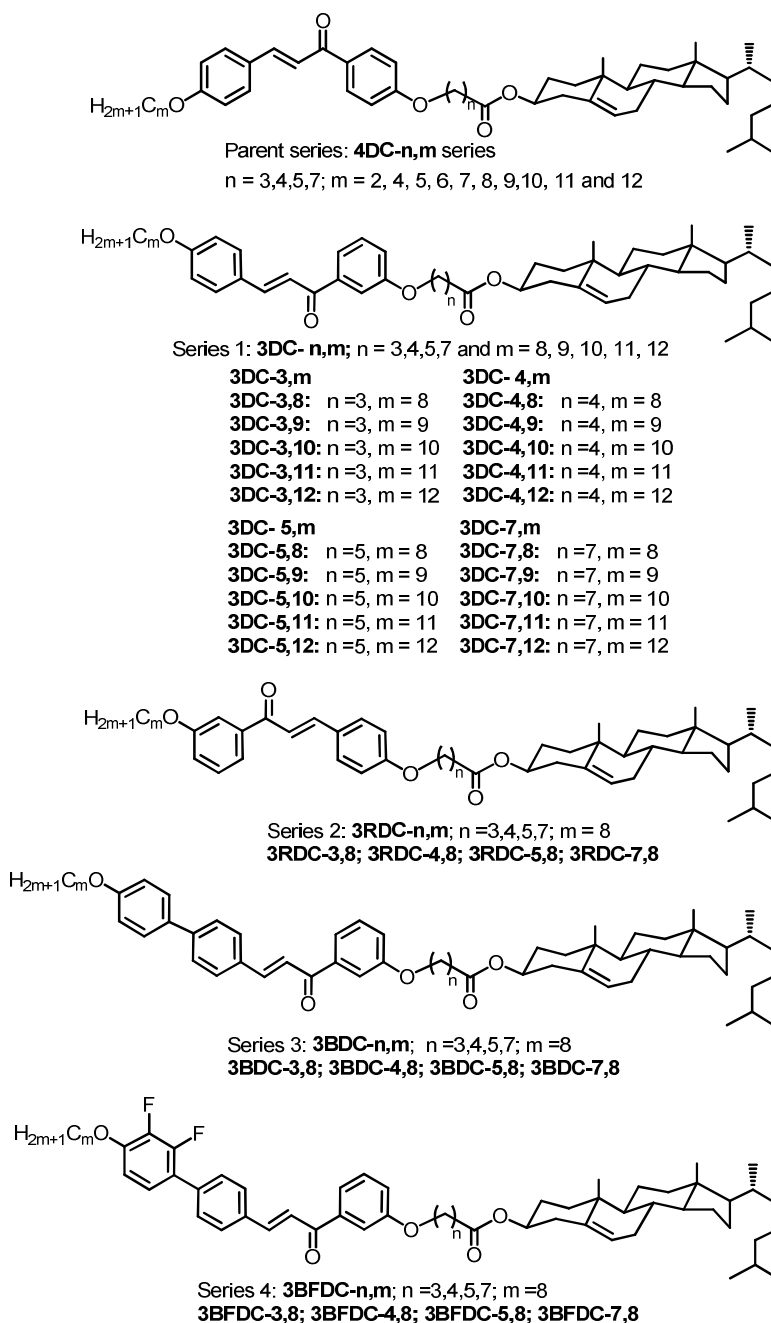


**Chart 1:** Molecular structures of cholesterol-based dimers belonging to previous (**4DC-n,m** series) and present (series **1-4**) studies.

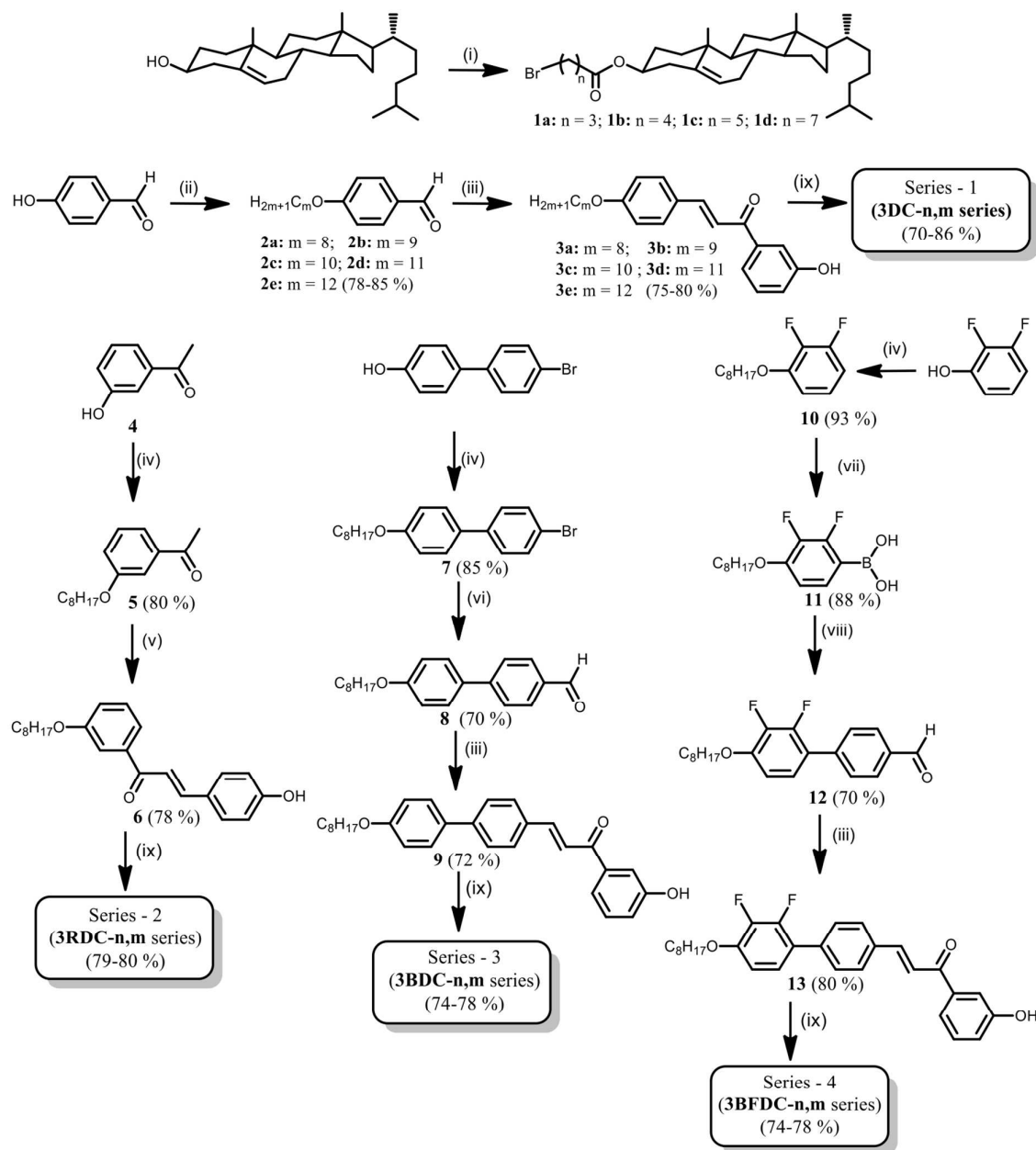
interactions and to visualize its effect on the thermal behaviour we have synthesized another series (Series 3: **3BDC-n**) where the long chalcone core (having abiphenyl ring) is joined to cholesterol through a spacer of varying length and parity. Owing to small size and high electro negativity, fluorine atom has long been used to generate lateral dipole, minimize viscosity, lower transition temperature as well as to alter the phase transitional behaviour of LCs.<sup>18,19</sup> Keeping these points in view, we realized another series of dimers (Series 4: **3BFDC-n**) where the lateral fluoro substituted, long-chalcone core is tethered to cholesterol via a spacer. Thus, in the four series of dimers realized, two primary structural modifications with respect to parent series were incorporated: (i) altered the relative positions of cholesteryloxycarbonyl-*n*-alkane and/or *n*-alkoxy tail attached to each of the two phenyl rings of chalcone (Series 1 and 2) and (ii) elongated one of the aryl rings with or without fluoro lateral substitutions of chalconering (Series 3 and 4).

## II. Results and discussion

### II.1 Synthesis and molecular structural characterization

The synthetic route adopted to prepare the target dimers and their precursors is outlined in scheme 1. Cholesteryl  $\omega$ -bromoalkanoates (**1a-d**) were synthesized by treating cholesterol with the freshly prepared 4-bromobutanoyl, 5-bromopentanoyl, 6-bromohexanoyl or 8-bromooctanoyl chlorides, as reported in the literature.<sup>20,21</sup> The key intermediates namely, hydroxy chalcones **3a-e**, **6**, **9** and **13** were prepared as described in the literature<sup>22</sup> wherein various alkaryl ketones were condensed with appropriate aldehydes in the presence of methanolic solution of KOH, which we briefly describe as follows. The requisite 4-(*n*-alkoxy)benzaldehydes **2a-e** were prepared by the *o*-alkylation of 4-hydroxybenzaldehyde with appropriate *n*-bromoalkane in butanone using anhydrous K<sub>2</sub>CO<sub>3</sub> as a mild base. These 4-*n*-alkoxybenzaldehydes (**2a-e**) were condensed with 3-hydroxyacetophenone to yield (*E*)-1-(3-hydroxyphenyl)-3-(4-*n*-alkoxyphenyl)prop-2-en-1-ones (**3a-e**). Compound **6**, (*E*)-3-(4-hydroxyphenyl)-1-(3-(octyloxy)phenyl)prop-2-en-1-one, was prepared starting from 3-hydroxyacetophenone, which was first *o*-alkylated with *n*-octylbromide in the presence of anhydrous K<sub>2</sub>CO<sub>3</sub> in butanone, followed by condensation of **5** with 4-hydroxybenzaldehyde. Subsequently, chalcone **9**, (*E*)-1-(3-hydroxyphenyl)-3-(4'-(*n*-octyloxy)biphenyl-4-yl)prop-2-





**Scheme 1.** Synthesis of four series of cholesterol-based dimers. Reagents and conditions: (i) *n*-Bromoalkanoyl chlorides, pyridine, THF, 0-5 °C to rt, 8 h; (ii) *n*-bromoalkane, anhydrous  $\text{K}_2\text{CO}_3$ , butanone, reflux,  $\text{N}_2$ , 12 h; (iii) 3-hydroxyacetophenone, KOH, methanol, reflux, 12 h; (iv) 1-bromooctane, anhydrous  $\text{K}_2\text{CO}_3$ , butanone, 80 °C, 12 h; (v) 4-hydroxybenzaldehyde, KOH, methanol, 60 °C, 12 h; (vi) *n*-BuLi, DMF, THF,  $\text{N}_2$ , -78 °C to rt, 12 h; (vii) (a) *n*-BuLi, triisopropyl borate, THF,  $\text{N}_2$ , -78 °C to rt, 12 h; (b) 10 % HCl (aq); (viii) 4-bromobenzaldehyde, 2M  $\text{Na}_2\text{CO}_3$  (aq) solution,  $\text{Pd}(\text{PPh}_3)_4$ , benzene, ethanol, reflux; (ix) **1a-d**, anhydrous  $\text{K}_2\text{CO}_3$ , DMF,  $\text{N}_2$ , 80 °C, 12 h.



en-1-one, was synthesized by reacting 4'-(*n*-octyloxy)biphenyl-4-carbaldehyde (**8**) with 3-hydroxyacetophenone. In turn, aldehyde **8** was prepared starting from 4'-bromobiphenyl-4-ol; it was *o*-alkylated with *n*-octylbromide in the presence of anhydrous K<sub>2</sub>CO<sub>3</sub> to obtain 4-bromo-4'-(*n*-octyloxy)biphenyl (**7**); this was lithiated using *n*-butyl lithium (*n*-BuLi) and thus, *in situ* generated aryllithium reagent was quenched with dry DMF to obtain 4-*n*-octyloxy-4'-biphenyl aldehyde (**8**) in 62 % yield. Next, the fluoro analogue **13**, (*E*)-3-(2',3'-difluoro-4'-(*n*-octyloxy)biphenyl-4-yl)-1-(3-hydroxy-phenyl)prop-2-en-1-one, of chalcone **9** was prepared in four steps as depicted in the scheme. 2,3-Difluorophenol was *o*-alkylated with *n*-bromooctane to get 1,2-difluoro-3-(*n*-octyloxy)benzene (**10**) in reasonably good yield. The aryllithium reagent generated by the reaction of compound **10** with *n*-BuLi in dry THF was treated with triisopropyl borate and thus, borate ester obtained was subjected to hydrolysis using 10% HCl (aqueous) to give 2,3-difluoro-4-(*n*-octyloxy)phenylboronic acid **11**. Palladium catalysed Suzuki cross-coupling reaction of arylboronic acid **11** with 4-bromobenzaldehyde furnished 2',3'-difluoro-4'-(*n*-octyloxy)biphenyl-4-carbaldehyde (**12**), which upon treating with 3-hydroxy acetophenone under basic reaction condition yielded chalcone **13**. Finally, the target dimers were prepared by *o*-alkylation of hydroxy chalcones **3a-e**, **6**, **9** and **13** with appropriate cholesteryl  $\omega$ -bromoalkanoates (**1a-d**) under typical Williamson ether synthesis conditions. The structures of all the intermediates and target molecules were confirmed using spectroscopic data and/or elemental analyses (see the supporting information for the details).

## II. 2. Thermal behavior

The mesomorphism of these new LC dimers belonging to four different series was investigated by polarizing optical microscope (POM), differential scanning calorimeter (DSC) and X-ray diffraction (XRD). The occurrence of thermotropic LC phase(s) was initially verified based on the observation of strong birefringence and fluidity under POM. Explicit LC phase assignment was made according to the characteristic textural pattern seen. The peak temperatures obtained in DSC traces due to phase transitions were found to be consistent with those of POM studies. The transition temperatures and the corresponding enthalpies derived from DSC traces of the first heating-cooling cycles at a rate of 5 °C/min are given. In the following sections, we present the details of LC behaviour of the dimers derived from the studies using above-mentioned complementary techniques.

## II. 2.1. Series 1 (3DC-n,m series)

As can be seen in Chart 1, in this series, the cholesterol is covalently linked to

**Table 1.** Transition temperatures ( $^{\circ}\text{C}$ )<sup>a</sup> and enthalpies (J/g) of 3DC-n,m series of dimers

Dimer	Phase sequence	
	Heating	Cooling
3DC-3,m		
3DC-3,8	Cr 115.4 <sup>b</sup> [16.5] N* 121.7 [3] I	I 120.7 [3] N* 93.4 [32.5] Cr
3DC-3,9	Cr 128.6 [62.9] I	I 120.7 [3.3] N* 100.9 [42.8] Cr
3DC-3,10	Cr 133.3 [63.8] I	I 118.9 [3.4] N* 107.5 [42.2] Cr
3DC-3,11	Cr 135.6 [57.5] I	I 116.2 [3.1] N* 111.9 [48.5] Cr
3DC-3,12	Cr 132.8 [62.8] I	I 118.2 [3.9] N* 111.6 [47.6] Cr
3DC-4,8	Cr 130.8 [82] I	I 80.5 [56.2] Cr
3DC-4,9	Cr 105.5 [63.9] I	I 78.4 [49.5] Cr
3DC-4,10	Cr 101.4 <sup>c</sup> [49.8] I	I 82.4 [42.4] Cr
3DC-4,11	Cr 107.3 [62.7] I	I 89.7 [58.3] Cr
3DC-4,12	Cr 118.5 [79.6] I	I 93.8 [55.5] Cr
3DC-5,8	Cr 97.9 [55.7] N* 110.8 [3.6] I	I 109.8 [3.5] N* 71.9 <sup>d</sup> TGB 57 <sup>d</sup> Cr
3DC-5,9	Cr 98 [55.2] N* 109.9 [3.8] I	I 108.9 [3.7] N* 82.8 <sup>d</sup> TGB 64 <sup>d</sup> Cr
3DC-5,10	Cr 99.9 [47] N* 109.2 [3.9] I	I 108.2 [3.8] N* 48.7 [14.9] Cr
3DC-5,11	Cr 105.8 [47.8] N* 108.1 [3.5] I	I 107.2 [3.4] N* 86.4 <sup>d</sup> TGBC* 68.2 [30.1] Cr
3DC-5,12	Cr 109.1 <sup>e</sup> [25.8] I	I 106.4 [4.3] N* 76.6 [0.5] TGBC* 72.6 [31.9] Cr
3DC-7,8	Cr 86.2 [59.5] N* 104.8 [4.4] I	I 104.1 [4.2] N* 84.8 <sup>d</sup> TGB 74 <sup>d</sup> SmA 42.2 [5] Cr
3DC-7,9	Cr 85.6 [62.5] N* 104.1 [4.6] I	I 102.9 [4.4] N* 78.6 <sup>d</sup> TGB 65.3 <sup>d</sup> SmA 43 <sup>d</sup> Cr
3DC-7,10	Cr 89.9 [64.2] N* 102.8 [4.3] I	I 101.9 [4.5] N* 77.3 <sup>d</sup> TGB 72.3 <sup>d</sup> SmA 39 <sup>d</sup> Cr
3DC-7,11	Cr 88.8 [64.2] N* 102.2 [4.5] I	I 101.5 [4.4] N* 73.6 <sup>d</sup> TGB 46 <sup>d</sup> Cr
3DC-7,12	Cr 94.7 [62.6] N* 104.4 [4.6] I	I 103.9 [4.7] N* 80.5 <sup>d</sup> TGBC* 61.1 [11.1] Cr

Cr = Crystal; N\* = Chiral nematic phase; TGB = twist grain boundary phase with smectic A (SmA) / smectic C (SmC) slabs; TGBC\* = twist grain boundary phase with SmC\* slabs. I = Isotropic liquid state (These abbreviations are applicable wherever mentioned)<sup>a</sup> Peak temperatures in the DSC thermograms obtained during the first heating and cooling cycles at 5  $^{\circ}\text{C} / \text{min}$ ; <sup>b</sup> A crystal to crystal transition was observed at 113.5  $^{\circ}\text{C}$  [10.7 J/g]; <sup>c</sup> A crystal to crystal transition was seen at 96  $^{\circ}\text{C}$  [19.4 J/g]. <sup>d</sup> The phase transition observed under POM was too weak to be detected by DSC; <sup>e</sup> Crystal to crystal transitions were observed at 75.1  $^{\circ}\text{C}$  [5 J/g] and 103.8  $^{\circ}\text{C}$  [37.3 J/g]

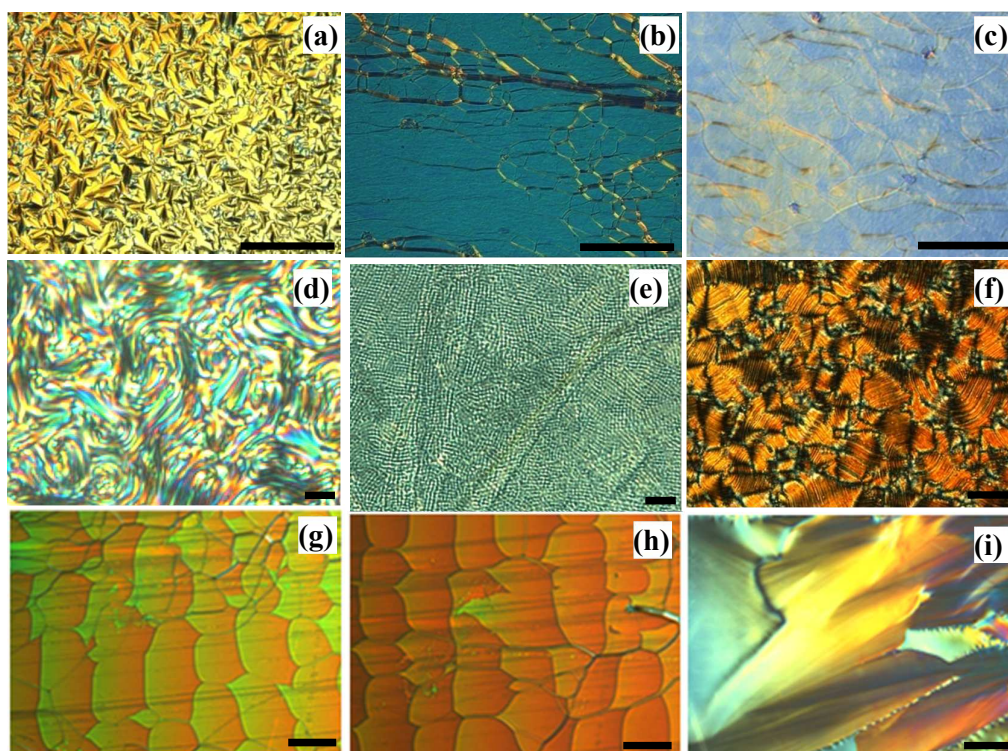


**Figure 2.** Photomicrographs of optical textures seen under POM for the LC phases of dimers of series-1 (**3DC-n,m** series): (a) focal-conic texture of the N\* phase seen at 117 °C while cooling **3DC-3,8** from the isotropic phase; (b) oily streak texture obtained upon shearing the focal-conic pattern of the N\* phase (at 117 °C) of **3DC-3,8**; (c) planar texture of the TGB phase formed at 71 °C on cooling the planarly aligned N\* phase of **3DC-5,9**; (d) filamentary texture seen for the TGB phase at 65 °C for the homeotropically aligned **3DC-5,9**; (e) square grid pattern of the TGBC\* phase seen for dimer **3DC-5,11** at 92°C; (f) texture of the TGBC\* phase grown at 72°C on top of focal-conic pattern of the N\* phase of **3DC-5,11**; (g) GC dislocation lines observed at 87 °C for the N\* phase of **3DC-7,8** ; (h) GC dislocation lines noticed at 82 °C for the TGB phase of **3DC-7,8** ; (i) focal-conic texture of the SmA phase existing just below the TGB phase (74 °C). (Bar: 100 μm).

chalcone through either trimethylene ( $n = 3$ ; 4-oxybutanoyl; even-parity) or tetramethylene ( $n = 4$ ; 5-oxybutanoyl; odd-parity) or pentamethylene ( $n = 5$ ; 6-oxyhexanoyl; even-parity) or heptamethylene ( $n = 7$ ; 8-oxyoctanoyl, even-parity) spacer; while the chalcone is substituted with  $n$ -octyloxy to  $n$ -dodecyloxy ( $m = 8$  to 12) tails. These structural variations give rise to four sub homologous (**3DC-3,m**, **3DC-4,m**, **3DC-5,m** and **3DC-7,m**) series of dimers. Thus, the thermal behavior (transition temperatures and enthalpies) of **3DC-3,m**, **3DC-4,m**, **3DC-**

**5,m** and **3DC-7,m** series of dimers comprising 4-oxybutanoyl, 5-oxyentanoyl, 6-oxyhexanoyl, and 8-oxyoctanoyl spacer is summarized in Table 1.

As can be seen, the dimers of **3DC-3,m** having 4-oxybutanoyl (even-parity) spacer exhibit chiral nematic (N\*) phase only. In particular, the N\* phase is enantiotropic for the first dimer **3DC-3,8**, while it is monotropic in higher members. Seemingly, this trend is in contrast to the general observation that in a given homologous series of low molar mass (monomeric) LCs the mesophases are often metastable for lower members, and only the higher homologues display enantiotropic behavior;<sup>1c,d</sup> the monotropic phase transitions of the lower homologues can be accounted for their higher melting temperature as cause of the reduced flexibility. The N\* phase was identified by optical textural observation. When examined under POM in the form of a thin film of sample prepared between two untreated glass slides and cooled from the isotropic phase (I), the focal-conic texture was obtained, which on mechanical stressing yielded an oily streaks pattern. The focal-conic and oily streaks textures, as shown in shown in Fig. 2a and Fig. 2b respectively, for dimer **3DC-3,8** as a representative case, are typical of the N\* phase. Compared to the occurrence of smectic A (SmA) and /or N\* phase(s) in dimers with an identical spacer of parent **4DC-n,m** series, these compounds exhibit only the N\* phase, which points to the importance of the position at which cholesteryloxycarbonyl-*n*-alkane is attached to chalcone in determining the phase behaviour. It may be noted here that **3DC-3,m** series of compounds display lower N\*-I or Cr-I transition temperature than those of analogous parent dimers implying the possibility of **3DC-3,m** series of molecules attaining bent conformation.

Contrary to expectation, none of the dimers belonging to **3DC-4,m** series exhibit mesomorphic behaviour (see Table 1) despite possessing pro-mesogenic cholesterol segment. However, the loss of mesomorphism in these dimers can be duly interpreted in terms of their pronounced bent molecular conformation and thus reduced shape anisotropy. Specifically, in these dimers the cholesterol and 4-*n*-alkoxychalcone anisometric segments are inclined with respect to each other as they are linked by an odd-parity (5-oxyentanoyl; C<sub>5</sub>) spacer. Thus, the overall molecular shape considered in all-*trans* conformation of these dimers (Fig. 3a) is bent as against to the linear shape of **3DC-3,m** series of dimers wherein the two mesogenic segments are separated by an even-parity spacer (Fig. 3b). It is important to remark here that when compared to a noteworthy thermal behaviour of parent series of compounds<sup>15h,i</sup> having a 5-oxyentanoyl spacer, especially the dimers with *n*-decyloxy to *n*-

dodecyloxy ( $m = 10$  to  $12$ ) tails,<sup>15h</sup> these **3DC-4,m** series of dimers fail to exhibit LC property.

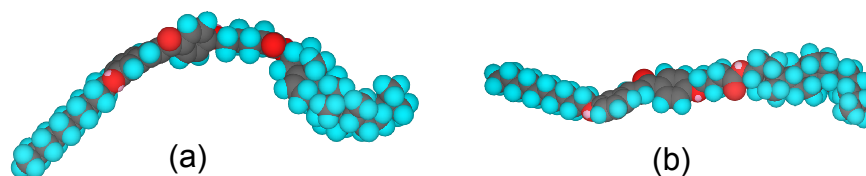


**Figure 3.** Energy minimized structures of dimers (a) **3DC-4,10** and (b) **3DC-3,10**. Note that mesogenic segments of the dimer **3DC-4,10** with an odd-parity spacer are inclined to each other.

It can be seen from Table 1 that the dimers of **3DC-5,m** series, wherein cholesterol and chalcone cores are separated by a 6-oxyhexanoyl (even-parity) spacer, show LC behaviour. The first two compounds *viz.*, **3DC-5,8** and **3DC-5,9** of the series exhibit an enantiotropic N\* phase in addition to a monotropic TGB phase. The existence of N\* phase was ascertained based on the textural observation; for example, when a thin film of the isotropic liquid of dimer **3DC-5,9** contained in either normal glass plates or substrates treated for planar alignment, was cooled slowly, a focal-conic texture was observed, which on mechanical shear changes to a planar pattern. On further cooling, Grandjean planar texture of the N\* phase transforms sharply to yet another but distinct deep gray blurry planar texture as shown in Fig. 2c. Such a planar pattern is reported to be seen for the TGB phase<sup>23-25</sup> in which the molecular long axes are parallel to the substrate and thus the smectic (SmA or SmC) layer planes are perpendicular to the glass plates. On cooling the sample further, the planar texture gradually converts to a blurred focal-conic texture. When the sample was subjected to homeotropic boundary condition to attain the long molecular axis orientation perpendicular to the substrates, the N\* and TGB phases showed the focal-conic and vague vermis (filamentary) (Fig. 2d) patterns respectively.<sup>24a</sup> All these optical observations clearly indicate that these two dimers exhibit a dimesomorphic sequence involving a transition from the N\* to the TGB phase. The occurrence of TGB phase over 15 °C thermal range is noteworthy in light of the fact that such phases being frustrated, are known to exist for short thermal range,<sup>4</sup> except for a few cases.<sup>15h,i</sup>



The next dimer **3DC-5,10** exhibits an enantiotropic N\* phase exclusively over a wide thermal range (about 60 °C) indicating that a slight variation (lengthening) of the terminal tail greatly influences the phase behaviour of these dimers. Based on the behaviour of dimer **3DC-5,10** it may be reasonable to presume that the higher members of this compound would continue to show the N\* phase. In contrast to this assumption, the next higher homologue **3DC-5,11** exhibit a monotropic TGBC\* phase besides the enantiotropic N\* phase. Surprisingly, these two phases were found to be metastable for the next higher dimer **3DC-5,12**. The occurrence of dimesomorphic sequence was adjudged based on the textural observation, which we briefly discuss for the dimer **3DC-5,11**. This dimer exhibits N\* phase with a planar texture in which the nematic director lies in the plane of the substrate. This ensures that the helical axis is perpendicular to the glass plates *i.e.*, along the viewing direction. On further cooling, the transition to another phase was noticed wherein the planar texture of the N\* phase sharply changes to a square grid pattern as shown in Fig. 2e, which is reported to be an important signature for the existence of a complex and highly frustrated mesophase, namely the twist grain boundary (TGB) phase possessing chiral smectic C (SmC\*) blocks, denoted as the TGBC\*<sup>15i-l, 25-28</sup>. According to Galerne's model of TGBC\* phase,<sup>25</sup> in addition to the tilt of the molecules with respect to the smectic layer normal, there is a precession of the SmC director, resulting in a second helix orthogonal to the TGB helix axis; consequently, each smectic block has a smectic C\* structure (Fig. 1e, right). A direct consequence of this is the appearance of square grid pattern. Experimentally, it has been observed that the TGBC\* phase indeed exhibits a square grid pattern superimposed on the planar texture as mentioned above. When the sample was examined in slides treated for homeotropic alignment and cooled from the focal-conic texture of the N\* phase, a non-specific texture consisting of some tiny undulated filaments was seen as shown in Fig. 2f. The occurrence of tiny grid pattern or indistinct undulated filaments perhaps implies that pitch of the helix is short. In comparison, the thermal behavior of these **3DC-5,m** series of dimers having a 6-oxyhexanoyl (even-parity) spacer is markedly different from the analogous parent dimers. As discussed above, except for dimer **3DC-5,12**, all the compounds display an enantiotropic mesophase; whereas, the corresponding dimers of parent series display metastable mesophases with the exception of compound having *n*-dodecyloxy tail. Interestingly, the dimer **3DC-5,12** displays two monotropic mesophases featuring helical structure while the analogous dimer of parent series stabilizes an enantiotropic layered mesophase, the SmA phase. It can be therefore inferred that these dimers have reduced shape anisotropy owing to their bent molecular shapes.

All the dimers with 8-oxyoctanoyl (even-parity) spacer of **3DC-7,m** series display an enantiotropic N\* phase in addition to one or two monotropic phases such as TGB, SmA and TGBC\* as summarized in the Table 1. The first three dimers viz., **3DC-7,8**, **3DC-7,9** and **3DC-7,10** exhibit an enantiotropic N\* phase as well as monotropic TGB and SmA phases that was ascertained by the optical textural observation. When a thin film of these dimers placed between a slide and a cover slip was cooled slowly from the isotropic phase, the transition to N\* phase occurs with characteristic focal-conic texture that on mechanical shear changes to planar pattern. Upon cooling the sample further from the Grandjean planar (oily streak) texture of the N\* phase, a transition to another mesophase takes place with a gray blurry planar texture, which is typical of the TGB phase. On further cooling, a phase transition was noticed with textural pattern consisting of blurred focal-conic fans accompanied by some planar regions of TGB phase. On lowering the temperature further, in some regions of the slide, especially at the edges, well-defined focal-conic fans typical of SmA phase were noticed. When these samples were examined between glass slides treated for homeotropic alignment, the N\* and TGB phases respectively showed the focal-conic and vague vermis (filamentary) patterns.<sup>24a</sup> In order to elucidate the phase sequence further, the dimer **3DC-7,8** as representative case, was investigated in a wedge type cell treated for planar orientation wherein the thickness varies from one end to other. On cooling the isotropic liquid, the Grandjean Cano (GC) dislocation lines (striations running from the top to bottom of the pattern) were observed for the N\* and TGB phase, as shown in Fig. 2g and Fig. 2h respectively, demonstrating that there is a helical twist normal to the plates in these phases.<sup>15h-i, 26</sup> On cooling the sample further from planar texture having GC dislocation lines of TGB phase, these dislocation lines become wider progressively, and disappear leaving behind only the planar pattern. Nearing the transition to SmA phase, the TGB phase exhibits a texture wherein the fine arcs, over the planar pattern move randomly and rapidly. When the transition to SmA phase takes place, this planar pattern transforms sharply into a texture consisting of focal-conic fans as shown in Fig.2i. Thus, these experimental results ascertain the existence of N\*, TGB (with either SmA or SmC slabs) and SmA phases in these dimers. As shown in Table 1, the dimers **3DC-7,11** and **3DC-7,12** with relatively longer terminal tails exhibit a dimesomorphic sequence involving a transition from N\* to TGB and N\* to TGBC\* phases, respectively. It is worth mentioning here that the above-mentioned phase sequences of these dimers, including the other series of materials, are highly reproducible that clearly demonstrate their thermal stability.



Within the series, the melting and clearing temperatures of these dimers seem not varying much as a function of terminal tail length; however, upon ascending the series, the smectic behaviour gets extinguished with exclusive occurrence of TGB phase. A general comparison of the phase behaviour of these dimers belonging to **3DC-7,m** series with those of analogous parent systems shows that they commonly exhibit N\* and frustrated phases with optional SmA phase; remarkably, the former dimers show TGB phase below the N\* phase while the latter ones display BP above the N\* phase. The melting and clearing temperatures of present series of dimers are at least 20 °C below the analogous parent systems indicating that the former systems are perhaps twisted to some extent.

**Table 2.** The results of indexation of XRD profiles of dimers at a given temperature (T) of mesophases; the estimated all-*trans* molecular length (*l*); layer spacings (*d*); *d/l* ratio and structural assignment of the smectic phases of dimers. SmC\*: chiral smectic C phase

Dimer	T(° C)	<i>d</i> (Å)	<i>l</i> (Å)	<i>d/l</i>	Nature of the phase
<b>3DC-7,8</b>	70	24.7 4.9	51	0.48	Intercalated SmA
<b>3RDC-3,8</b>	122	45.1 22.3 5.1	47	0.96	Monolayered SmA
	60	43.8 5	47		SmC*(tilt angle 21.6°)
<b>3BDC-7,8</b>	145	26.3 5.1	54	0.49	Intercalated SmA
<b>3FDC-7,8</b>	100	25.2 5	53	0.48	Intercalated SmA

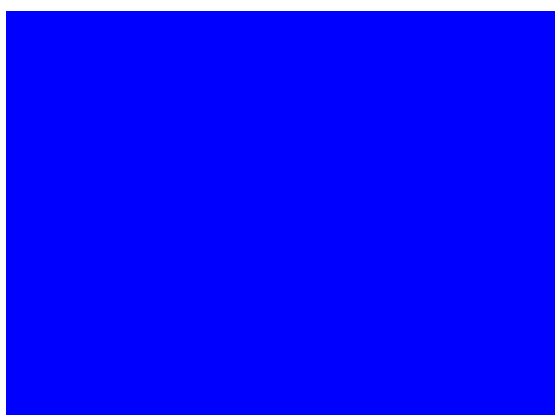


**Figure 4.** A schematic representation of the self-assembly of dimer **3DC-7,8** into an intercalated SmA phase. Notice that the terminal alkyl chains and the spacers are mixed.

It is now well documented that the structure (periodicity) of the SmA phase formed by cholesterol-based dimers decisively depends upon the relative lengths of the spacer and terminal chains.<sup>10a, 11-15, 29</sup> Thus, the SmA phase of dimer **3DC-7,8**, in which the length of the terminal tail and spacer are equal, was investigated by powder X-ray diffraction (XRD), as a representative case. The results of indexation of XRD profile is summarized in Table 2. The diffractogram obtained at 70 °C showed a sharp peak in the low angle region with a  $d$ -value of 24.7 Å that can be attributed to originating from the layered structure. Besides, a typical diffuse scattering in the wide angle region ( $d = 4.9$  Å) was observed pointing to the liquid like order within the smectic layers. The calculated length of the molecule ( $l$ ) using a Chem3D molecular model is 50.61 Å. Thus the  $d/l$  ratio is 0.49, which points to the formation of an intercalated SmA phase as shown in Fig. 4. It can therefore be inferred that cholesterol-based dimers stabilize an intercalated SmA phase if they possess terminal tail and flexible spacer of equal length.

Thus, among the four sub series of dimers synthesized, all the five compounds of **3DC-4,m** series having odd-parity spacer are nonmesomorphic, while other three homologous series of compounds viz., **3DC-3,m**, **3DC-5,m** and **3DC-7,m** formed by varying the length of even-parity spacer are liquid crystalline. It is quite apparent from the comparison of the thermal behaviour of these three series of dimers that the nature and extent of mesomorphism is dependent on the length of the even-parity spacer. For example, all the homologues of **3DC-3,m** series exhibit N\* phase and the thermal range of this phase decreases with increase in the length of the terminal chain. In **3DC-5,m** series, except for dimer with *n*-decyloxy tail which exhibits only the N\* phase, all the compounds stabilize frustrated mesophases like TGB or TGBC\* besides the N\* phase; interestingly, the alternation of the N\*-TGB or N\*-TGBC\* transition temperature as a function of number of carbon atoms in the terminal chain occurs. Within the **3DC-7,m** series of dimers, the length of the terminal tail influences the phase behaviour; the dimers with *n*-octyloxy to *n*-decyloxy tails stabilize a trimesomorphic sequence viz., N\*-TGB-SmA while compounds comprising *n*-undecyloxy and *n*-dodecyloxy chains display a dimesomorphic sequence involving a transition from N\* to TGB/TGBC\* phase; here also a marginal transition temperature alternations as a function of the length of the terminal chain persists. A common feature of these three sets of compounds is that within each series the isotropic liquid to mesophase transition temperature remains more or less the same regardless of the terminal chain length. It may also be noted here that the LC to isotropic liquid phase transition temperature reduces

progressively upon lengthening the spacer. Contrary to the occurrence of blue phase in vast majority of the dimers of parent series, none of these dimers display such a frustrated structure. Therefore, in comparison to the parent series, these dimers showed different thermal behaviour, thus signifying the fact that even a small variation in the molecular structure will lead to a dramatic change in the mesomorphic behavior of chiral dimers. This clearly indicates that the stabilization of the frustrated phases involves a delicate balance between the length, parity, and position of attachment of spacer, structure of the aromatic mesogenic unit and the length of the terminal chain.

## II. 2.2. Series 2 (3RDC-*n,m* series)

In this series of dimers, as compared to materials belonging to **3DC-*n,m*** series, the positions of *n*-alkoxy tail and cholesteryloxy carbonyl-*n*-alkane substituents of chalcone are interchanged. In other words, the chalcone linkage is reversed that perhaps imparts different (linear) conformation to the molecule when compared to the members of **3DC-*n,m*** series. Thus, it would be interesting to compare the thermal behaviour of **3RDC-*n,m*** series of dimers with that of **3DC-*n,m*** series. Table 3 gives the transition temperatures and associated enthalpies of these four dimers belonging to **3RDC-*n,8*** series. From the results it can be seen that the dimer **3RDC-4,8** having an odd-parity (5-oxypentanoyl) spacer is nonmesomorphic

**Table 3.** Transition temperatures ( $^{\circ}\text{C}$ )<sup>a</sup> and enthalpies (J/g) of **3RDC-*n,m*** series

SmA = Smectic A /SmC\* = smectic C phase (applicable wherever mentioned)

Dimer <b>3RDC-<i>n,8</i></b>	Phase sequence	
	Heating	Cooling
<b>3RDC-3,8</b>	Cr 117.3 [42.2] SmA 135.3 [9.5] I	I 132.6 [9.4] SmA 64 <sup>b</sup> SmC* 42 <sup>c</sup> Cr
<b>3RDC-4,8</b>	Cr 107.1 [45.6] I	I 92.4 [42.8] Cr
<b>3RDC-5,8</b>	Cr 100.7 [38.9] SmA 114.4 <sup>b</sup> TGB 118.4 [1.5] N* 122.5 [2.5] I	I 121.6 [2.4] N* 117.3 [1.3] TGB 113.6 <sup>b</sup> SmA 66.1 <sup>b</sup> SmC* <sup>d</sup>
<b>3RDC-7,8</b>	Cr 102.1 [1.1] N* 113.3 [3.7] I	I 112.2 [3.2] N* 100 <sup>b</sup> TGB 88 <sup>b</sup> SmA 88.8 [46.3] Cr

<sup>a</sup> Peak temperatures in the DSC thermograms obtained during the first heating and cooling cycles at 5  $^{\circ}\text{C}/\text{min}$ . <sup>b</sup> The phase transition was observed under polarizing microscope and was too weak to be recognized by DSC. <sup>c</sup> The SmA-Cr phase transition observed with a microscope was too weak to be detected by DSC. <sup>d</sup> The mesophase freezes into glassy state instead of crystallization.

that can be ascribed to pronounced bent conformation and thus, reduced shape anisotropy of the molecule; this is analogous to the behaviour of dimer **3DC-4,8**. On the other hand, dimers **3RDC-3,8**, **3RDC-5,8** and **3RDC-7,8** composed of even-parity spacer exhibit mesomorphic behavior, which we briefly describe as follows. The dimer **3RDC-3,8** placed between two glass slides treated for planar anchoring condition and cooled slowly from the isotropic liquid, a striking focal-conic texture typical of the SmA phase was obtained. On cooling the sample further, dechiralization lines appeared on the top of the focal conic

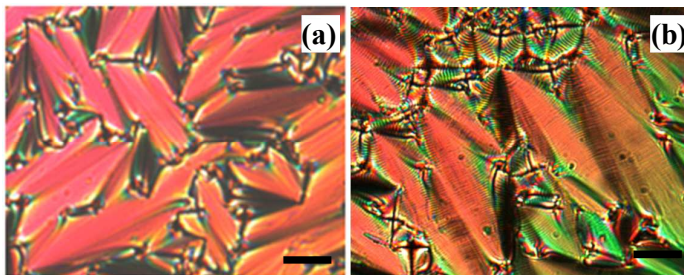


**Figure 5.** Photomicrographs of the focal conic texture of the SmA phase (80.7 °C) (a) and focal conics with chiral lines obtained for SmC\* phase (50 °C) of the dimer **3RDC-5,8** (b) (Bar: 100  $\mu\text{m}$ ).

texture, characteristic of the SmC\* phase. As expected, in slides treated for homeotropic orientation the SmA and SmC\* phases displayed the *pseudo*-isotropic and cloudy textures, respectively. It may be recalled here that **3DC-3,8**, the positional isomer of this dimer **3RDC-3,8**, displays an enantiotropic N\* phase solely indicating that interchanging the relative positions of *n*-alkoxy tail and cholesteryloxycarbonyl-*n*-alkane substituents of chalcone influences the phase behaviour significantly. The dimer **3RDC-5,8** displays enantiotropic N\*, TGB and SmA phases besides a monotropic SmC\* phase. This polymesomorphic sequence was established based on the microscopic textural observation. Upon cooling the compound (taken between ordinary slides) from isotropic phase a focal conic texture appears for the N\* which on shearing yielded a Grandjean planar texture; on cooling further (from planar texture) TGB phase appears with planar textural pattern. On lowering the temperature further, focal-conic texture, as shown in Fig. 5a, typical of the SmA phase was seen. When this phase was cooled further, a partially aligned focal-conic fan texture featuring dechiralization lines on top of it characteristic of the SmC\* phase was observed (Fig. 5b). Upon lowering the temperature further, the sample did not crystallize, instead the SmC\* phase was found to be non-shearable at  $\sim 40$  °C; this perhaps

indicates the freezing of the SmC\* phase into a glassy state. The DSC traces corroborated these observations where no peak was seen till  $-60^{\circ}\text{C}$ . In addition, the SmC\* phase of this dimer was investigated for the ferroelectric switching characteristics by the method already described before. Surprisingly, contrary to our expectation, no electrical switching was observed. Even with quite large voltages, there was no sign of switching, and moreover, the sample could not sustain such high field strengths limiting further investigations. Thus, **3RDC-5,8** exhibits a poly mesomorphic sequence *viz.*, N\*-TGB-SmA-SmC\*, while in comparison, the isomeric dimer **3DC-5,8** of previous series shows a dimesomorphic (N\*-TGB) sequence. Compound **3RDC-7,8** displays the N\*-TGB-SmA phase sequence where the latter two phases were found to be monotropic in nature. Remarkably, the TGB phase exists for a thermal range of 18 degrees.

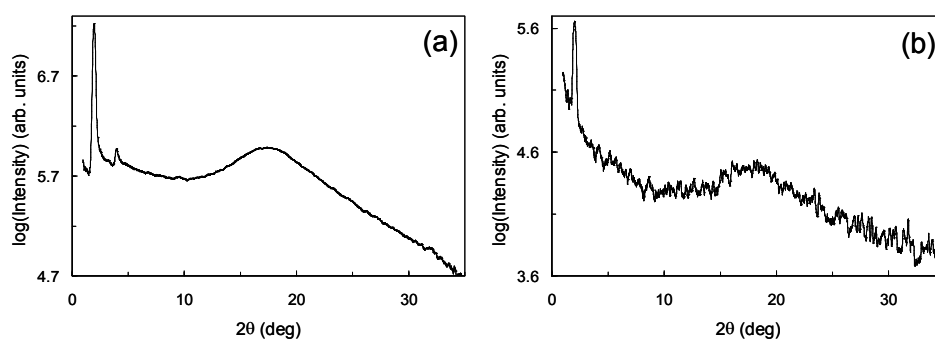


**Figure 6.** The intensity vs  $2\theta$  profiles extracted from the XRD patterns of the SmA phase at  $122^{\circ}\text{C}$  (a) and SmC\* phase at  $60^{\circ}\text{C}$  (b) for the dimer **3RDC-3,8**.

In order to provide more insight into the SmA and SmC\* phases formed by dimer **3RDC-3,8**, XRD experiments were carried out. The X-ray intensity profiles obtained in the SmA phase at  $122^{\circ}\text{C}$  and SmC\* at  $60^{\circ}\text{C}$  phase are presented in Figures 6a and 6b respectively. The XRD data deduced from these profiles are summarized in Table 2. It can be seen that the low angle region of the diffractograms consists of two sharp reflections with  $d$ -values  $45.1\text{ \AA}$  and  $22.3\text{ \AA}$  for the SmA phase (Fig. 6a) and a sharp reflection at  $43.8\text{ \AA}$  for the SmC\* phase (Fig. 6b). In addition, the diffractograms of SmA and SmC\* phases show a diffuse peak in the wide angle region with  $d$ -values  $5.1\text{ \AA}$  and  $5\text{ \AA}$  respectively, which can be attributed to the intermolecular separation within the layer arising due to the liquid-like positional correlation of the flexible alkyl tails. The reflection at  $22.3\text{ \AA}$  seen for SmA phase is the second harmonic which is generally observed for the dimeric systems and originates from the part of the molecule.<sup>10a</sup> The calculated length in the most extended form of all-*trans*

configuration of the molecule ( $l$ ), measured using Chem3D molecular model is 47 Å. Hence the  $d$ -value 45.1 Å obtained for the SmA phase nearly corresponds to the length of the molecule ( $l$ ), with the  $d/l$  ratio of 0.95 which is characteristic of monolayer SmA phase. Whereas, the layer spacing in SmC\* with  $d = 43.8$  Å, as expected, is less than the estimated all-*trans* molecular length,  $l = 47$  Å, which indicate the tilted organization of the molecules within the smectic layers. The tilt angle,  $\theta$ , of the molecules in this SmC\* phase with respect to the layer normal was estimated to be  $\sim 21.6^\circ$  using the expression,  $\theta = \cos^{-1}(d/l)$ . In general, these dimers with chalcone linkage connected in a reverse fashion favour the formation of layered mesophases. Indeed, the length and parity of the spacer play an important role in dictating the mesophase behaviour of these dimers.

### II. 2. 3. Series 3 (3BDC-*n,m* series)

The phase sequences, transition temperatures and associated enthalpies of dimers of **3BDC-*n,m*** series are summarized in Table 4. It must be noted here that these four dimers are rather different from those of parent series or the three series of compounds described above; they possess an elongated chalcone core where one of the phenyl rings is substituted with a biphenyl ring. Thus, the overall molecular length of these dimers is increased and consequently, as compared to other three series of dimers described earlier, their clearing temperatures are higher. It is also important to mention here that the length and parity of the central spacer is varied while terminal chain of the chalcone is kept constant with *n*-octyloxy tail. The first member **3BDC-3,8** of the series having an 4-oxybutanoyl, (even-parity) spacer exhibits enantiotropic N\* and TGB phases besides a monotropic SmA phase. The striking filamentary texture seen while heating from a homeotropic aligned SmA phase is shown in Fig. 7a. When compared to monomesomorphic (N\*) and dimesomorphic (SmA-SmC\*) behaviour of dimers **3DC-3,8** and **3RDC-3,8** respectively, this material stabilizes a trimesomorphic sequence namely N\*-TGB-SmA. Interestingly, the next dimer **3BDC-4,8** comprising an 5-oxypentanoyl (odd-parity) spacer, unlike the analogous dimer belonging to **3DC-*n,m*** and **3RDC-*n,m*** series, display mesomorphism; in particular, it shows the N\* phase and BPs. On slow cooling the isotropic liquid, a mesophase appears at 154.7 °C with a bluish foggy texture of low birefringence without any structure in it, as shown in Fig. 7b. Such a texture is reported to be seen for the BPIII phase which is an amorphous phase and has the same symmetry as that of the isotropic phase.<sup>3c, 24a</sup> On further cooling, a platelet texture

composed of red, green and blue plates over the foggy pattern appears at 152.7 °C (Fig. 7c); this suggests the existence of a cubic blue phase which can be either BPI or BPII.<sup>24a</sup> These cubic blue phases are composed of ‘double twist cylinders’ which represent a local structure of minimum free energy. It is may be noted here that when sheared, both high and low temperature BPs display the characteristic Grandjean planar texture of the N\* phase. On lowering the temperature, BPI/BPII phase transforms into the N\* phase at 146.7 °C. Thus, the low and high temperature BPs occur over thermal ranges of 6 and 2 degrees respectively which is worth mentioning given the reason that such phases, being highly frustrated structures, exist over a very narrow temperature interval.

**Table 4.** Transition temperatures (°C)<sup>a</sup> and enthalpies (J/g) of **3BDC-n, 8** series

BPIII = Blue phase III; BP = Blue phase I / II (applicable wherever mentioned)

Dimer	Phase sequence	
	Heating	Cooling
<b>3BDC-3,8</b>	Cr 138.7 [54] TGB 147.2 <sup>b</sup> N* 183 [3] I	I 181.9 [2.8] N* 146.2 <sup>b</sup> TGB 127 <sup>b</sup> SmA 62 <sup>b</sup> Cr
<b>3BDC-4,8</b>	Cr 135.3 <sup>c</sup> [33.9] N* 157.2 [2.6] I	I 154.7 [1.1] BPIII 152.7 BP 146.7 [1.1] N* 111.9 [27.3] Cr
<b>3BDC-5,8</b>	Cr 104.2 [29.7] SmA 148.4 <sup>b</sup> TGB 154.7 [0.3] N* 171.2 [3.6] I	I 165.2 [3.4] N* 152.3 <sup>b</sup> TGB 145.6 [0.3] SmA 84.1 <sup>b</sup> Cr
<b>3BDC-7,8</b>	Cr 99.8 [31.1] SmA 152.6 <sup>b</sup> TGB 155.6 [2.1] N* 162.9 [3.9] I	I 159.7 [3.8] N* 153 <sup>b</sup> TGB 149.8 [1.8] SmA 65 <sup>d</sup>

<sup>a</sup> Peak temperatures in the DSC thermograms obtained during the first heating and cooling cycles at 5 °C/min; <sup>b</sup> The phase transition was observed under polarizing microscope and was too weak to be recognized by DSC; <sup>c</sup> A crystal to crystal transition was observed at 120.9 [27.6]; <sup>d</sup> The phase freezes at 65 °C.

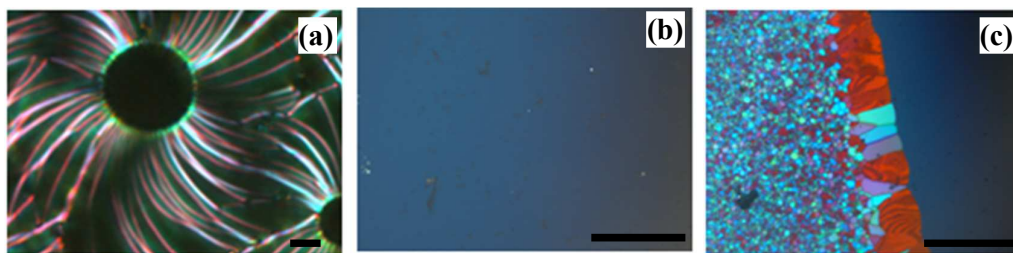


**Figure 7.** (a) The filamentary texture of TGB phase growing around the air packets of homeotropic SmA phase (at 148 °C) of dimer **3BDC-3,8**; (b) the foggy texture of BPIII obtained at 153 °C for dimer **3BDC-4,8**; (c) platelet texture of cubic blue phase (either BPI or BPII) obtained at 152 °C for dimer **3BDC-4,8**. (Bar: 100 μm).



The dimers **3BDC-5,8** and **3BDC-7,8** composed of 6-oxyhexanoyl and 8-oxyoctanoyl spacer, respectively, exhibit N\*, TGB and SmA phases in a manner reminiscent of the thermal behavior of first member **3BDC-3,8** of the series having an 4-oxybutanoyl, (even-parity) spacer. Thus, dimers of this series having even-parity spacer behave identically with the exception of clearing temperature that decreases with increase in spacer length. A comparison of the phase behaviour of **3BDC-5,8** with dimers **3DC-5,8** and **3RDC-5,8** shows that all of them commonly stabilize N\* and TGB phases, while the occurrence and the extent of smectic behavior appear to be dependent on the nature of the chalcone segment they possess. Interestingly, the thermal behaviour of dimer **3BDC-7,8**, and **3DC-7,8** and **3RDC-7,8** is identical indicating that the dimers possessing 8-oxyoctanoyl spacer are insensitive to the variations in structure of chalcone mesogenic segment. As a representative case, the SmA phase formed by dimer **3BDC-7,8** was investigated by XRD technique. The diffractogram obtained at 145 °C showed a sharp reflection with  $d = 26.3 \text{ \AA}$  and a diffused peak at wide angle with  $d$  value of  $5.1 \text{ \AA}$  (Table 2). The latter is characteristic of liquid-like order within the smectic planes. The sharp peak at  $26.3 \text{ \AA}$  represents the layer thickness, with a value much less than the estimated molecular length ( $l$ ) of  $54 \text{ \AA}$  and thus, the  $d/l$  ratio is 0.49. This ratio is the characteristic of an intercalated SmA phase. It is appropriate to recall here that the dimer **3DC-7,8**, having the spacer and terminal tail of equal lengths, as in dimer **3BDC-7,8**, also exhibits an intercalated SmA phase.

#### II. 2. 4. Series 4 (3FDC-n,m series)

Table 5 presents the LC behaviour of four dimers of **3FDC-n,m** series where the cholesterol moiety is covalently linked to the laterally fluoro substituted chalcone core through an  $\omega$ -oxyalkanoyl spacer of varying parity and length. The energy-minimized models of these dimers show that the terminal phenyl ring of chalcone remain out of plane when compared to co-planar organization in their non-fluoro analogues, the **3BDC-n,m** series of dimers. As we discussed at the beginning, lateral fluoro-substituents in rigid (*e.g.* biphenyl or terphenyl) cores help in reducing the melting point of the parent system.<sup>18,19</sup> Thus, these dimers are expected to show the reduced transition temperatures. It may also be reasonable to assume that the lateral substitution of the biphenyl ring with fluorine atom can direct the molecules to pack feebly during their self-assembly. Needless to mention that such a packing reduces the phase transition temperatures. As anticipated, the members of **3FDC-n,m** series show slightly lower transition temperatures when compared to that of **3BDC-n,m** series of dimers (see Table 5). Furthermore, with respect to parity of the alkylene spacer these

dimers exhibit odd-even effect in clearing temperatures, which is in agreement with the results presented above for the other series of dimers. That is the dimer **3FDC-3,8** having a relatively shorter spacer, the 4-oxybutanoyl (even-parity) spacer, has the highest clearing temperature followed by the dimers **3FDC-5,8** and **3FDC-7,8** having 6-oxyhexanoyl and 8-oxyoctanoyl spacers respectively. Indeed, the dimer **3FDC-4,8** exhibits lowest clearing temperature as it contains an odd-parity (5-oxy-pentanoyl) spacer.

**Table 5.** Transition temperatures ( $^{\circ}\text{C}$ )<sup>a</sup> and enthalpies (J/g) of **3FDC - n,8** series

Dimer	Phase sequence	
	Heating	Cooling
<b>3FDC-3,8</b>	Cr 132.4 <sup>b</sup> [43.1] N* 168.8 [12.3] I	I 164.6 [12] N* 116.5 <sup>c</sup> TGBC* 105.5 <sup>c</sup> Cr
<b>3FDC-4,8</b>	Cr 127.6 [56.2] N* 139.8 [2.9] I	I 137.5 [2.4] BPIII 133.2 <sup>c</sup> N* 87.1 [16] Cr
<b>3FDC-5,8</b>	Cr 110.6 [52.1] SmA 118.2 TGB 140.2 [2.4] N* 158.2 [3.6] I	I 155 [3.5] N* 136.4 <sup>c</sup> TGB [2.3] 115 <sup>c</sup> SmA 52.6 <sup>d</sup>
<b>3FDC-7,8</b>	Cr 96.3 [32.9] SmA 119.5 <sup>c</sup> TGB 121.5 <sup>c</sup> N* 147 [4] I	I 146.8 [3.8] BP 145.2 <sup>c</sup> N* 121 <sup>c</sup> TGB 118 <sup>c</sup> SmA 54.6 <sup>c</sup> Cr

<sup>a</sup> Peak temperatures in the DSC thermograms obtained during the first heating and cooling cycles at 5  $^{\circ}\text{C}/\text{min}$ . <sup>b</sup> Additional crystal-crystal transition is observed at 110.6 [26.8]. <sup>c</sup>The phase transition was observed under polarizing microscope and was too weak to be recognized by DSC. <sup>d</sup> The mesophase freezes into the glassy state.

In general, all the dimers stabilize an enantiotropic N\* phase. The first dimer **3FDC-3,8** displays a monotropic TGBC\* phase additionally; the presence of this phase was figured out by the observation of square grid pattern on top of the planar texture of the N\* phase. In comparison with thermal behaviour of analogous dimer **3BDC-3,8**, compound **3FDC-3,8** disfavours the formation of smectic phase. Notably, the next dimer **3FDC-4,8** displays BPIII over a thermal range of 4 degrees above the N\* phase, which is identical to the phase behaviour of its non-fluoro analogue, the dimer **3BDC-4,8**. The dimers **3FDC-5,8** and **3FDC-7,8** display enantiotropic SmA, TGB and N\* phases, while the latter compound stabilizes the BPI/II additionally. When the dimer **3FDC-7,8** was cooled gradually (0.2  $^{\circ}\text{C}$ ) from the isotropic phase in the form of a thin film, a platelet texture characteristic of BPI/BPII was observed. Upon cooling the sample further or subjecting to mechanical stress, the platelet texture transforms to the N\* phase exhibiting a brightly colored texture having oily streaks. On lowering the temperature, the transitions to TGB and SmA phases occur as established by the observation of blurred planar and focal conic textures, respectively. For the homeotropic alignment, these SmA and TGB phases displayed *pseudo*-isotropic and filamentary patterns respectively. It is appropriate to mention here that when homeotropically

aligned sample was heated between the rate of 5-10 °C/min, the N\* and SmA phases coexisted along with the TGB phase as evident from the fact that the textures corresponding to these three mesophases appeared simultaneously for a short while. Thus, dimers **3FDC-5,8** and **3FDC-7,8** commonly display enantiotropic SmA, TGB and N\* phases, which is reminiscent of the phase behaviour of dimers **3BDC-5,8** and **3BDC-7,8**.

To determine the structure of the SmA phase, XRD measurement was carried out on an unoriented sample **3FDC-7,8**, as a representative case. The results derived from the XRD diffractogram are summarized in Table 2. The 1D-intensity vs  $2\theta$  profile showed a sharp peak in the low angle region and a diffuse peak in the wide-angle region with spacings 25.2 Å and 5 Å respectively. While the diffuse peak is typical of liquid-like order within the smectic planes, the sharp peak at 25.2 Å corresponds to the layer thickness and it is nearly half the value of the estimated molecular length  $l \sim 53$  Å implying that dimers between neighbouring layers interdigitate. This result is in agreement with the fact that the cholesterol-based dimers such as **3DC-7,8** and **3BDC-7,8** having the spacer and terminal tail of equal lengths form an intercalated SmA phase. Recently, there was also a report, where the achiral unsymmetrical dimers with an even-parity spacer exhibit intercalated smectic phase due to the specific interaction between the unlike mesogenic segments.<sup>30</sup> We assume that this interaction also contributes to the formation of intercalated SmA phase.

### III. Summary

Thirty-two new optically active nonsymmetric dimers belonging to four series have been synthesized and investigated for their thermal behaviour. These dimers comprise promesogenic cholesterol and short bent-core chalcone, interlinked covalently through an  $\omega$ -oxyalkanoyl spacer of varying length and parity. Fundamentally, these four series of compounds differing in the structure of the chalcone were prepared with the aim of comparing their thermal behaviour with that of the known dimers of identical nature, referred to as parent dimers. Our study clearly reveals the thermal behavioural differences between the new dimers and parent systems.

The dimers of the first series, which are the positional isomers of parent systems, in turn constitute four sub-series wherein cholesterol is covalently tethered to 4-*n*-alkoxy-3'-hydroxychalcone using either 4-oxybutanoyl or 5-oxypentanoyl or 6-oxyhexanoyl or 8-oxyoctanoyl spacer. Within the series, the length of the flexible terminal tail varies from *n*-

octyloxy to *n*-dodecyloxy. The dimers of the first sub-series with 4-oxybutanoyl (even-parity) spacer, in contrast to the polyomesomorphic or only the smectic behaviour of parent analogues, exhibit only the N\* phase; this indicates the importance of the position at which cholesteryloxycarbonyl-*n*-alkane is attached to chalcone in determining their phase behaviour. Within this series, the variation of the length of the terminal tail seems to have almost no effect on the I-N\* phase transition temperature. The dimers of second sub-series with an odd-parity (5-oxy-pentanoyl) spacer, contrary to expectation, did not show any LC phase; this can be attributed to the pronounced bent-conformation and thus reduced shape anisotropy of the molecules. The dimers of third sub-series having 6-oxyhexanoyl (even-parity) spacer stabilize an enantiotropic N\* phase; except for the dimer possessing *n*-dodecyloxy tail, all of them also display a monotropic TGB / TGBC\* phase. Within the series, the increase in the length of terminal chain appears to have no much effect on Cr-N\*, N\*-I or I-N\* phase transition temperatures; instead, it determines the type of frustrated phase to be formed. The first two dimers possessing *n*-octyloxy and *n*-nonyloxy tails display TGB phase (which may have either SmA or SmC slabs), while the other two compounds with *n*-undecyloxy and *n*-dodecyloxy tails stabilize TGBC\* phase. Moreover, the alternation of the N\*-TGB or N\*-TGBC\* transition temperature (during cooling) as a function of number of carbon atoms in the terminal chain occurs. In the dimers of fourth sub-series in which the cholesterol and chalcone entities are joined covalently through an 8-oxyoctanoyl spacer, the length of the terminal tail influences the phase behaviour. The dimers with *n*-octyloxy to *n*-dodecyloxy tails stabilize N\*, TGB and SmA phases while compounds comprising *n*-undecyloxy and *n*-dodecyloxy chains display a sequence involving transition from N\* to TGB/TGBC\* phase; here also a marginal transition temperature alternations as a function of the length of the terminal chain persists. The XRD study on the SmA phase of dimer having *n*-octyloxy tail confirmed the intercalated organization of the molecules within the phase. Most importantly, these four series of compounds display a different behaviour compared to parent systems clearly indicating the dependence of phase transitional properties of cholesterol-based dimers on the nature of the rod-like (non-cholesteryl) mesogen; the study also confirms dramatic dependence of their transitional properties on the length and parity of the spacer.

In the second series, as compared to parent systems or the members of first series, the chalcone ( $\alpha,\beta$ -unsaturated ketone) linkage is reversed imparting extended linear conformation to the molecules. It is a rather short series, where the length of the terminal tail *viz.*, *n*-

octyloxy, is kept constant while the length and parity of the spacer is varied. Three dimers having an even-parity spacer exhibit mesophases whereas the compound with an odd-parity (5-oxyptanoyl) spacer is nonmesomorphic. The dimer with 4-oxybutanoyl spacer displays SmA and SmC\* phases for which the monolayer and tilted monolayer arrangements of the molecules were evidenced by XRD study. The compound having 6-oxyhexanoyl spacer exhibits the sequence N\*-TGB-SmA-SmC\*, while in the dimer with 8-oxyoctanoyl spacer, the SmC\* phase is suppressed.

The dimers belonging to the third series are different from those of parent series or the two series of materials described above. That is they possess an elongated chalcone where, one of the aryl rings is substituted with a 4-*n*-octyloxybiphenyl instead of phenyl ring. Interestingly, all of them are mesomorphic; stabilization of BPIII, BPI/II and N\* phases by the dimer possessing an odd-parity (5-oxyptanoyl) spacer is noteworthy in view of the fact that the compounds of other series with an analogous spacer are crystalline. The other three dimers having 4-oxybutanoyl or 6-oxyhexanoyl or 8-oxyoctanoyl spacer exhibit N\*, TGB and SmA phases. The occurrence of the intercalated SmA phase for the dimer consisting of an 8-oxyoctanoyl spacer was established by XRD measurement. The increase in the spacer length seems to reduce the Cr-SmA/N\*, N\*-I or I-N\* transition temperatures. In general, the thermal behaviour of these compounds agrees with that of the parent dimers.

The fourth series of dimers, which are the fluoro analogues of dimers of third series, display mesomorphic behavior with the expected lower transition temperatures. In this series also, the dimer with odd-parity spacer is mesomorphic exhibiting BP and N\* phase. For the members with even-parity spacer, the number of mesophases increases on lengthening the spacer; the dimers with 4-oxybutanoyl, 6-oxyhexanoyl and 8-oxyoctanoyl spacers show respectively the sequences: N\*-TGBC\*, N\*-TGB-SmA and BP-N\*-TGB-SmA.

In essence, the study clearly illustrates the complex interplay of the different molecular sub-units of the dimers in stabilizing mesophases such as blue phase(s), chiral nematic, twist grain boundary, smectic A and chiral smectic C phases.

### Acknowledgements

CVY sincerely thanks Science and Engineering Board (SERB), DST, Govt. of India for funding this work through the project No. SR/S1/OC-04/2012

## References

1. (a) S. Chandrasekhar, *Liquid Crystals*, 2nd ed.; Cambridge University Press: New York, 1994; (b) P. G. De Gennes and J. Prost, *The Physics of Liquid Crystals*; Oxford Science Publication: Oxford, 1993; (c) J. W. Goodby, P. J. Collings, T. Kato, C. Tschierske, H. Gleeson and P. Raynes, Eds.; *Handbook of Liquid Crystals: Fundamentals*, Wiley-VCH: Weinheim, Germany, 2014; Vol. 1; (d) J. W. Goodby, I. M. Saez, S. J. Cowling, V. Görtz, M. Draper, A. W. Hall, S. Sia, G. Cosquer, S. -E. Lee and E. P. Raynes, *Angew. Chem. Int. Ed.*, 2008, **47**, 2754; (e) T. Geelhaar, K. Griesar and B. Reckmann, *Angew. Chem. Int. Ed.* 2013, **52**, 8798; (f) C. Tschierske, *Angew. Chem. Int. Ed.* 2013, **52**, 8828.
2. F. Renitzer, *Monatsh. Chem.* 1888, **9**, 421.
3. (a) I. Sage, In *Liquid Crystals: Applications and Uses*; B. Bahadur, Ed; World Scientific: Singapore, 1992; Vol. 3, Chapter 20. (b) Q. Li (Ed), *Nanoscience with Liquid Crystals: From Self-Organized Nanostructures to Applications*, Springer, 2014. (c) Q. Li (Ed.), *Liquid Crystals Beyond Displays: Chemistry, Physics, and Applications*, John Wiley & Sons, 2012; (d) E.-K. Fleischmann and R. Zentel, *Angew. Chem. Int. Ed.* 2013, **52**, 8810; (e) M. Bremer, P. Kirsch, M. Klasen-Memmer and K. Tarumi, *Angew. Chem. Int. Ed.* 2013, **52**, 8880.
4. (a) S. R. Renn and T. C. Lubensky, *Phys. Rev. A.*, 1988, **38**, 2132; (b) P. G. de Gennes, *Solid State Commun.*, 1972, **10**, 753; (c) H.-S. Kitzerow and C. Bahr, *Chirality in Liquid Crystals*; Springer-Verlag, Inc.: New York, 2001; (d) J. W. Goodby, *Curr. Opin. Colloid Interface Sci.*, 2001, **7**, 326. (e) J. W. Goodby, M. A. Waugh, S. M. Stein, E. Chin, R. Pindak and J. S. Patel, *Nature*, 1989, **337**, 449; (f) J. W. Goodby, M. A. Waugh, S. M. Stein, E. Chin, R. Pindak and J. S. Patel, *J. Am. Chem. Soc.*, 1989, **111**, 8119. (g) J. W. Goodby, In *Structure and Bonding: Liquid Crystals II*; D. M. P. Mingos, Ed.; Springer-Verlag: Berlin, 1999; p 83.
5. (a) S. T. Lagerwall, In *Ferroelectric and Antiferroelectric Liquid Crystals*; S. T. Lagerwall, Ed; Wiley-VCH: Weinheim, Germany, 1999; (b) D. M. Walba, *Science*, 1995, **270**, 250. (c) S. Garoff, R. Meyer, *Phy. Rev. Lett.*, 1977, **38**, 848-851; (d) S. T. Lagerwall, M. Matuszyk, P. Rodhe and L. Odma, In *The Optics of Thermotropic Liquid Crystals*; S. J. Elston, J. R. Sambles, Eds.; Taylor and Francis: London, 1998.

6. (a) Z. Ge, S. Gauza, M. Jiao, H. Xianyu and S. T. Wu, *Appl. Phys. Lett.* 2009, **94**, 101104. (b) J. Yan, L. Rao, M. Jiao, Y. Li, H. C. Cheng and S. T. Wu, *S. T. J. Mater. Chem.* 2011, **21**, 7870. (c) Y. H. Lin, H. S. Chen and T. H. Chiang, *J. Soc. Inf. Disp.* 2012, **20**, 333. (d) J. Yan, S. T. Wu, K. L. Cheng and J. W. Shiu, *Appl. Phys. Lett.* 2013, **102**, 081102. (e) Y. Chen and S. T. Wu, *Appl. Phys. Lett.* 2013, **102**, 171110. (f) H. J. Coles and S. Morris, *Nat. Photonics* 2010, **4**, 676. (g) W. Cao, A. Munoz, P. Palffy-Muhoray, and B. Taheri, *Nature Mater.* 2002, **1**, 111. (h) F. Castles, F.V. Day, S. M. Morris, D-H. Ko, D. J. Gardiner, M. M. Qasim, S. Nosheen, P.J.W. Hands, S. S. Choi, R. H. Friend and H. J. Coles, *Nature Mater.* 2012, **11**, 599. (i) T.-H. Lin, Y. Li, C.-T. Wang, H.-C. Jau, C.-W. Chen, C.-C. Li, H. Krishna Bisoyi, T. J. Bunning, and Q. Li, *Adv. Mater.* 2013, **25**, 5050. (j) H. J. Coles and M. N. Pivnenko, *Nature*, 2005, **436**, 997. (k) H. Kikuchi, M. Yokota, Y. Hisakado, H. Yang and T. Kajiyama, *Nature Mater.* 2002, **1**, 64.
7. (a) C. T. Imrie, in *Structure and Bonding - Liquid crystals, II*, Ed: Mingos, D. M. P., Springer-Verlag., **1999**, p.149. (b) C. T. Imrie and P. A. Henderson, *Curr. Opin. Colloid Interface Sci.*, **2002**, **7**, 298. (c) C. T. Imrie, and P. A., Henderson, *Chem. Soc. Rev.*, **2007**, **36**, 2096. (d) C. T. Imrie and G. R. Luckhurst, in *Handbook of liquid crystals., Vol-2B*, Eds: Demus, D., Goodby, J. W., Gray, G. W., H. -W. Spiess, and V. Vill, Weiley-VCH, Germany., **1998**, part – III, p.799.
8. V. Borshch, Y.-K. Kim, J. Xiang, M. Gao, A. Jaklil, V.P. Panov, J. K. Vij, C. T. Imrie, M.G. Tamba, G.H. Mehl and O.D. Lavrentovich, *Nature Communications*, 2013, **4**, 2635.
9. (a) D. S. Shankar Rao, S. Krishna Prasad, V. N. Raja, C. V. Yelamaggad and S. A. Nagamani, *Phy. Rev. Lett.*, 2001, **87**, 085504(1-4); (b) C. V. Yelamaggad, M. Mathews, T. Fujita, and N. Iyi, *Liq. Cryst.*, 2003, **30**, 1079; (c) C. V. Yelamaggad, U. S. Hiremath, D.S. Shankar Rao and S. Krishna Prasad, *Chem. Commun.* 2000, 57.
10. (a) C. V. Yelamaggad, G. Shanker, U. S. Hiremath and S. K. Prasad, *J. Mater. Chem.*, 2008, **18**, 2927 and the references cited therein; (b) C. T. Imrie, P. A. Henderson, G.-Y. Yeap, *Liq. Cryst.*, 2009, **36**, 755.



11. (a) F. Hardouin, M. F. Achard, J. -I. Jin, J. W. Shin and Y. K. Yun, *J. Phys. II Fr.*, 1994, **4**, 627; (b) F. Hardouin, M. F. Achard, J. -I. Jin and Y. K. Yun, *J. Phys. II Fr.*, 1995, **5**, 927; (c) F. Hardouin, M. F. Achard, J. -I. Jin, Y. K. Yun and S. J. Chung, *Eur. Phys. J.*, 1998, **B1**, 47.
12. (a) S.-W. Cha, J.-I. Jin, M. Laguerre, M. F. Achard and F. Hardouin, *Liq. Cryst.*, **1999**, **26**, 1325; (b) F. Hardouin, M. F. Achard, M. Laguerre, J. -I. Jin and D. H. Ko, *Liq. Cryst.*, **1999**, **26**, 589; (c) D. W. Lee, J. -I. Jin, M. Laguerre, M. F. Achard and F. Hardouin, *Liq. Cryst.*, 2000, **27**, 145; (d) S.-W. Cha, J. -I. Jin, M. F. Achard and F. Hardouin, *Liq. Cryst.*, 2002, **29**, 755; (e) J. -W. Lee, Y. Park, J. -I. Jin, M. F. Achard and F. Hardouin, *J. Mater. Chem.*, 2003, **13**, 1367; (f) K. -N. Kim, E. -D. Do, Y. -W. Kwon and J. -I. Jin, *Liq. Cryst.*, 2005, **32**, 229.
13. (a) A. T. M. Marcelis, A. Koudijs and E. J. R. Sudholter, *Recl. Trav. Chim. Pays-Bas*, 1994, **113**, 524; (b) A. T. M. Marcelis, A. Koudijs, and E. J. R. Sudholter, *Liq. Cryst.*, 1995, **18**, 843.
14. (a) A. T. M. Marcelis, A. Koudijs, E. A. Klop and E. J. R. Sudholter, *Liq. Cryst.*, 2001, **28**, 881 and references cited therein; (b) A. T. M. Marcelis, A. Koudijs, Z. Karczmarzyk and E. J. R. Sudholter, *Liq. Cryst.*, 2003, **30**, 1357.
15. (a) C. V. Yelamaggad, A. Srikrishna, D. S. Shankar Rao, S. K. Prasad, *Liq. Cryst.*, 1999, **26**, 1547; (b) C. V. Yelamaggad, *Mol. Cryst. Liq. Cryst.*, 1999, **326**, 149; (c) C. V. Yelamaggad, S. A. Nagamani, D. S. Shankar Rao, S. K. Prasad and U. S. Hiremath, *Mol. Cryst. Liq. Cryst.*, 2001, **363**, 1; (d) C. V. Yelamaggad, U. S. Hiremath, D. S. Shankar Rao, *Liq. Cryst.*, 2001, **28**, 351; (e) C. V. Yelamaggad, S. A. Nagamani, U. S. Hiremath, G. G. Nair, *Liq. Cryst.*, 2001, **28**, 1009; (f) C. V. Yelamaggad, M. Mathews, *Liq. Cryst.*, 2003, **30**, 125. (g) C. V. Yelamaggad, I. Shashikala, U. S. Hiremath, D. S. Shankar Rao and S. Krishna Prasad, *Liq. Cryst.*, 2007, **34**, 153; (h) C. V. Yelamaggad, A. S. Achalkumar, N. L. Bonde, and A. K. Prajapati, *Chem. Mater.*, 2006, **18**, 1076; (i) C. V. Yelamaggad, A. S. Achalkumar, N. L. Bonde, A. K. Prajapati, D. S. S. Rao, and S. K. Prasad, *Chem. Mater.*, 2007, **19**, 2463; (j) K. C. Majumdar, P. K. Shyam, D. S. S. Rao and S. K. Prasad, *J. Mater. Chem.*, 2011, **21**, 556; (k) A. S.

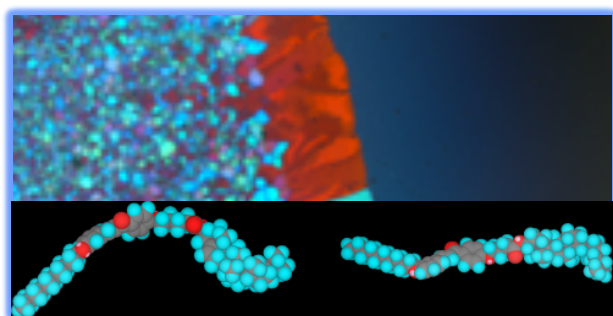
- Pandey, R. Dhara, A.S. Achalkumar and C.V. Yelamaggad, *Liq. Cryst.*, 2011, **38**, 775.(l) G. Shanker and C. V. Yelamaggad, *New J. Chem.*, 2012, **36**, 918.
16. G. S.Lim, B. M. Jung, S. J. Lee, H. H.Song, C. Kim and J. Y.Chang, *Chem. Mater.*, 2007, **19**, 460 and references cited therein.
17. (a) W. Tam, B. Gucrium, J. C. Calabreso and S. U. Sterenson, *Chem. Phys. Lett.*, 1989, **154**, 93; (b) J. Indira, P. P. Karat and B.K. Sarojini, *J. Crystal Growth*, 2002, **242**, 209; (c) X.T. Tao, T. Watanabe, K. Kono, T. Deguchi, M. Nakayama and S. Miyata, *Chem. Mater.* 1996, **8**, 1326.
18. (a) V. Bezborodoc, R. Dabrowski, J. Dziaduszek, K. Czuprynski and Z. Raszewski, *Liq. Cryst.*, 2006, **33**, 1487; (b) M. Hird and K. J. Toyne, *Mol. Cryst. Liq. Cryst.*, 1998, **323**, 1; (c) T. Hiyama, *Organoflourine Compounds; Chemistry and Applications*: Springer-Verlag Berlin Heidelberg, New York, 2000.
19. (a) G. W. Gray, M. Hird, D. Lacey and K. J. Toyne, *J. Chem. Soc. Perkin Trans II.*, 1989, 2041; (b) M. E. Gledening, J. W. Goodby, M. Hird and K. J. Toyne, *J. Chem. Soc. Perkin Trans II.*, 1999, 481; (c) M. E. Gledening, J. W. Goodby, M. Hird, D. Lacey and K. J. Toyne, *J. Chem. Soc. Perkin Trans II.*, 2000, 27; (d) M. Hird, J. W. Goodby and K. J. Toyne, *Proc. SPIE.*, 2000, **3955**, 15; (e) W.-K. Lee, K. -N. Kim, M. F. Achard and J.-I. Jin, *J. Mater. Chem.*, 2006, **16**, 2289.
20. I. W. Hamley, V. Castelletto, P. Parras, Z. B. Lu, C. T. Imrie and T. Itoh, *Soft Matter*, 2005, **1**, 355 and references cited therein.
21. V. Surendranath, *Mol. Cryst. Liq. Cryst.*, **1999**, 332, 135.
22. N. K. Chudgar and S. N. Shah, *Liq. Cryst.*, 1989, **4**, 661.
23. S.-W. Cha, J. -I. Jin, M. F. Achard and F. Hardouin, *Liq. Cryst.*, 2002, **29**, 755.
24. (a) I. Dierking, *Textures of Liquid Crystals*, Wiley-VCH Verlag GmbH & KGaA, Weinheim 2003; (b) I. Dierking and S. T. Lagerwall, *Liq. Cryst.*, 1999, **26**, 83.
25. Y. Galerne, *Eur. Phys. J. E.*, 2000, **3**, 355.

26. C. V. Yelamaggad, U. S. Hiremath, D. S. Shankar Rao and S. K. Prasad, *Chem. Commun.*, 2000, 57.
27. C. V. Yelamaggad, A. S. Nagamani, U. S. Hiremath, D. S. Shankar Rao and S. K. Prasad, *Liq. Cryst.*, 2001, **28**, 1581.
28. C. V. Yelamaggad, S. A. Nagamani, U. S. Hiremath, D. S. Shankar Rao and S. K. Prasad, *J. Chem. Res.*, 2001, 493.
29. W.-K. Lee, K.-N. Kim, M. F. Achard, J. -I. Jin, *J. Mater. Chem.*, 2006, **16**, 2289 and references cited therein.
30. G.-Y. Yeap, T.-C. Hng, S.-Y. Yeap, E. Gorecka, M. M. Ito, K. Ueno, M. Okamoto, W. Ahmad, K. Mahmood, C. T. Imrie, *Liq. Cryst.*, 2009, **36**, 1431.

Dr. A. S. Achalkumar  
Assistant Professor  
Department of Chemistry  
Indian Institute of Technology Guwahati  
Guwahati – 781039, Assam, India  
Phone: +91-361-258-2329  
Fax: +91-361-258-2349  
E-mail: achalkumar@iitg.ernet.in  
achalkumar78@gmail.com



## TOC contents



Nonsymmetric chiral dimers comprising chalcone and cholesterol entities have been prepared and studied for their structure property relations.